Available online at www.sciencedirect.com
SCIENCE DIRECT
International Journal of Heat and Mass Transfer 49 (2006) 649–657
International Journal of HEAT and MASS TRANSFER
www.elsevier.com/locate/ijhmt

An experimental and theoretical study on the concept of dropwise condensation

S. Vemuri, K.J. Kim *

Department of Mechanical Engineering, University of Nevada, Reno, NV 89557, USA

Received 28 September 2004; received in revised form 18 August 2005
Available online 2 November 2005

Abstract

Hydrophobic coatings have been created through self-assembled mono layers (SAMs) of *n*-octadecyl mercaptan (SAM-1) and stearic acid (SAM-2) on copper alloy (99.9% Cu, 0.1% P) surfaces to enhance steam condensation through dropwise condensation. When compared to complete filmwise condensation, *n*-octadecyl mercaptan (SAM-1) coated surface increased the condensation heat transfer rate by a factor of 3 for copper alloy surfaces, under vacuum condition (33.86 kPa) and to about eight times when operated under atmospheric condition (101 kPa). A model using the population balance concept is used to derive a theoretical formula to predict the drop-size distribution of small drops which grow mainly by direct condensation. All the important resistances to heat transfer such as the heat conduction through the drop, vapor–liquid interface are considered in developing this model. By knowing the contact angle of the drop made with the condensing surface and the maximum drop radius the sweeping effect of large falling drops could be calculated which is also incorporated into the model. The effect of interfacial heat transfer coefficient on heat transfer rate is also considered in developing the theoretical model. This is combined with the well known size distribution for large drops proposed by Le Fevre and Rose [E.J. Le Ferve, J.W. Rose, A theory of heat transfer by dropwise condensation, in: Proceedings of 3rd International Heat Transfer Conference, vol. 2, Chicago, 1966, pp. 362–375] which grow mainly by coalescence. There has been a satisfactory agreement between our experimental data and the present theoretical model.

Keywords: Dropwise condensation; Organic coatings; Mono-layers; Population balance

1. Objective

The main objective of the current research is to evaluate the effect of using self-assembled mono-layers (SAM's) technique for promoting dropwise condensation (DWC) and for enhancing condensation heat transfer rates. In the process a theoretical approach is derived for predicting the heat transfer rate in steam condensation during DWC and the results obtained from the theoretical model are compared with the experimental results obtained by using SAM's for promoting DWC for the validity of the model. In general, a SAM system with a long-chain, hydrophobic group is nano-resistant, meaning that such a system forms a protective hydrophobic layer with negligible heat transfer resistance. These mono-layers appear to offer a strong potential for long-term DWC promoters along with their low manufacturing costs involved. A model using the population balance concept [1–3] was used to derive a theoretical formula to predict the drop size distribution of small drops which grow mainly by direct condensation. All the important resistances to heat transfer such as the heat conduction through the drop, vapor–liquid interface are considered in developing this model. By knowing the contact angle of the drop made with the condensing surface and the maximum drop radius the sweeping effect of large falling drops could be calculated which is also incorporated into the model. The prior models [1–7] have not considered some of the various effects such as varying from different

* Corresponding author. Tel.: +1 775 784 7522; fax: +1 775 784 1701.
E-mail address: kwangkim@unr.edu (K.J. Kim).

0017-9310/$ - see front matter © 2005 Elsevier Ltd. All rights reserved.
doi:10.1016/j.ijheatmasstransfer.2005.08.016

Nomenclature

A	area of an arbitrary section on the condensing surface (m^2)
A_d	area swept by the large falling drop (m^2)
A_o	outside area of the test tube (m^2)
A_i	inside area of the test tube (m^2)
c_p	specific heat (J/kg K)
d_i	inside diameter of tube (m)
d_o	outside diameter of tube (m)
g	gravitational force (m/s^2)
G	growth rate (m/s)
h_i	interfacial heat transfer coefficient (W/m^2 K)
h_c	condensation heat transfer coefficient (W/m^2 K)
H_{fg}	latent heat of vaporization (J/kg)
h_w	tubeside heat transfer coefficient (W/m^2 K)
k_c	condensate thermal conductivity (W/m K)
K_1	constant in Eq. (25)
K	thermal conductivity of the tube (W/m K)
l	length of the tube (m)
n	population density of small drops (m^{-3})
N	population density of large drops (m^{-3})
N_s	number of nucleation sites on the condensing surface (m^{-2})
Nu	Nusselt number ($h_c l/\lambda$) as defined in Eq. (31)
Pr	Prandtl number ($c_p\mu/\lambda$) as defined in Eq. (31)
Q	heat flux of dropwise condensation (W/m^2)
q	rate of heat transfer (W)
r	drop radius (m)
r_{min}	minimum drop radius that can grow (m)
r_{max}	maximum drop radius (m)
$\hat{r}$	effective drop radius (m)
r_e	drop radius equal to half the spacing between the nucleation sites (m)
Re	Reynolds number (ul/v) as defined in Eq. (31)
SAM-1	*n*-octadecyl mercaptan coated surface
SAM-2	stearic acid coated surface
S	surface renewal rate due to sweeping of large falling drops (m^2/s)
t	time (s)
ΔT_d	temperature drop due to conduction through the drop (K)
ΔT_i	temperature drop due to interfacial resistance (K)
T_o	outlet water temperature (K)
T_i	inlet water temperature (K)
T_s	vapor temperature (K)
ΔT_{LMTD}	log mean temperature difference (K) as defined in Eq. (29)
ΔT	surface sub-cooling temperature (K)
u	coolant velocity (m/s)
U	overall heat transfer coefficient (W/m^2 K)

Greek symbols

ρ	density of the condensate (kg/m^3)
θ	contact angle
σ	surface tension (N/m)
v	kinematic viscosity (m^2/s)
λ	thermal conductivity of the condensate (W/m K)
μ	viscosity (N s/m^2)

operating pressures (from vacuum to atmospheric), sweeping effect of large falling drops, coalescence of drops, the actual surface area swept by falling drops and interfacial heat transfer coefficient for modeling in the process of dropwsie condensation. Interfacial heat transfer coefficient value increases as the operating pressure increases in the absence of non-condensable gases [8] which in turn increases the heat transfer rate in steam condensation and is also considered in developing the model. In developing the model the resistance due to drop curvature has been neglected since its effect is very small when compared to that of the resistances due to heat transfer such as the heat conduction through the drop and vapor–liquid interface. The resistance due to promoter layer is neglected in developing the model as the thickness of the SAM layer is very small (≈27 Å). This is combined with the well known size distribution for large drops proposed by Le Fevre and Rose [5] which grow mainly by coalescence. The data obtained from this theoretical model is compared to that of the data obtained from our experimentation. There has been a satisfactory agreement between our experimental data and the present theoretical model. Though the concept of promoting DWC using SAM's looks promising the durability of these surfaces need to be determined for any industrial applications. A detailed study of the prior techniques used for enhancing heat transfer rate in steam condensation both experimentally and theoretically are explained in the literature review.

2. Literature review

Condensation is still one of the most important heat transfer processes in many energy conversation systems. Condensers used in most of the real world applications are huge in size and are very expensive to manufacture. Any progress made in enhancing the condensation heat transfer rate would greatly reduce the driving potential or reduced pumping power required for desired output and finally the possibility of size reduction for the particular heat exchanger. Dropwise condensation (DWC) exhibits a significantly higher heat transfer coefficient [9,10] than filmwise condensation (FWC) when properly promoted. However, long term DWC conditions are usually difficult to maintain. Over the years many researchers have used

different techniques to enhance heat transfer in steam condensation both theoretically and experimentally, some of them are discussed below.

Fatica and Katz [4] were first to propose a model to compute the rate of heat transfer. They assumed that on a given area all drops are the same size, are uniformly spaced and grow by direct condensation. In later attempts, different researchers have dealt with the problem of drop-size distribution in a variety of ways. Wu and Maa [1] used the population balance method to derive the drop size distribution of small drops which grow mainly by direct condensation based on the assumption of steady size distribution. They estimated a vapor side heat transfer coefficient of dropwise condensation by assuming heat conduction through the drop as the only resistance to drop growth. Maa [2] used the population balance method to derive the drop size distribution of small drops which grow mainly by direct condensation. The number of nucleation sites was varied so that the result would fit the experimental data. Later, Abu-Orabi [3] modified the concept used by Maa [2] by incorporating the resistance due to the promoter layer into his model. Mousa has derived a theoretical derivation for the sweeping period in his model but, actually the sweeping period could be determined experimentally by knowing the maximum drop radius and the contact angle it made with the condensing surface. Mousa also assumed a radius slightly greater than that of the minimum radius which was not clearly explained. Le Fevre and Rose [5] derived a time-averaged distribution which had the correct behavior for the limiting cases of very large and very small drops. Rose and Glicksman [6] proposed a universal form of the distribution function for large drops which grow primarily by coalescence with smaller drops. The predicted distribution was not valid for small drops which grow by direct condensation. Rose [7] tried to improve the form by incorporating the resistances to heat transfer due to the drop and various contact angles. He suggested changing the radius of the smallest viable drop or the maximum drop radius or adding a resistance due to the promoter layer to match the experimental data. Tanaka [11,12] proposed a theory based on transient condensation and derived a set of simultaneous intergo-differential equations from statistical and geometrical considerations. The solutions of these equations were expressed in terms of four dimensional parameters, which were adjusted to fit the experimental data.

Erb and Thelen [13] have used coatings of inorganic compounds such as metal sulfides and found out that a sample of sulfided silver on mild steel showed excellent DWC. Extensive studies were made by researchers [14,15] on condensation by using noble metal plated surfaces and showed that noble metal plated surfaces have consistently showed excellent dropwise characteristics. However, the hydrophobic characteristics of these noble metals as DWC promoters have been controversial in the literature [16], and also the cost incurred in manufacturing such surfaces have limited their applications. Organic materials [17–19] like hydrocarbons and polyvinylidene chloride coatings had also received considerable attention for their hydrophobic capabilities to promote DWC. Many researchers [20–22] have used different types of technologies to employ polymer coatings for promoting DWC and reported that heat transfer enhancements were up to 30 times higher than film condensation. Das et al. [23] used an organic mono-layer coating and they concluded that SAM coatings increased the condensation heat transfer coefficient by a factor of 4. However, the durability of the coated surfaces has not been determined. In general, organic coatings are difficult to maintain, and require strong, long term adhesion forces between the coating and the metal substrate.

3. Model development

The derivation of the steady state distribution for small drops within the size range of negligible coalescence is based on the conservation of the number of drops in a given size range with no accumulation; i.e. the number of drops entering a size range must equal the number rate leaving.

As small drops grow by direct condensation from the smallest viable radius to the radius at which coalescence takes place, drops go through different sizes. If an arbitrary size range r_1 to r_2 is considered, then for the number of drops to be conserved in that size range, the number of drops entering by growth, must equal the number by growth and the number swept by large drops falling. The growth rate for a drop is defined as [1,24]:

$$G = \frac{\mathrm{d}r}{\mathrm{d}t} \tag{1}$$

The growth rate of a drop of radius r_1 is G_1 and that of a drop of radius r_2 is G_2, with letting the population density of drops be n_1 and n_2 for radiuses r_1 and r_2, respectively. Where n is the number of drops per unit area per unit drop radius. For a differential increment of time $\mathrm{d}t$, the number of drops entering this range because of growth is $An_1G_1\,\mathrm{d}t$. Similarly, the number of drops leaving by growth is $An_2G_2\,\mathrm{d}t$ ('A' is the area of an arbitrary section on the condensing surface in m^2). Drops in this size range are also removed by the sweeping flow of large falling drops. The number swept by falling drops is $S\bar{n}\,\Delta t\,\Delta r$, where S is the rate at which the substrate surface is renewed due to sweeping. If $\bar{n}$ is the average population density in the size range r_1 and r_2 with $\Delta r = r_2 - r_1$. Since the input to this range equals the output, the number of drops balance in the size range r_1 to r_2 gives: number of drops entering = number of drops leaving + number of drops swept,

$$An_1G_1\,\mathrm{d}t = An_2G_2\,\mathrm{d}t + S\bar{n}\,\Delta r\,\mathrm{d}t \tag{2}$$

Rearranging and dividing by $\mathrm{d}t$, the above equation gives

$$A(G_2n_2 - G_1n_1) = -S\bar{n}\,\Delta r \tag{3}$$

As Δr approaches zero, $\bar{n}$ becomes the point value and Eq. (2) takes the form,

$$\frac{\mathrm{d}}{\mathrm{d}r}(Gn) + \frac{n}{\tau} = 0 \tag{4}$$

where $\tau = A/S$.

The growth rate G of a single drop is derived by considering all the resistances (Fig. 1) to the heat transfer through the drop. Those resistances are expressed as a temperature difference as shown below:

$$\Delta T_{\mathrm{d}} = \frac{qr}{4\pi r^2 k_{\mathrm{c}}} \tag{5}$$

Vapor–liquid interfacial resistance for a hemispherical drop is given by [25,26],

$$\Delta T_{\mathrm{i}} = \frac{q}{2\pi r^2 h_{\mathrm{i}}} \tag{6}$$

where h_{i} is the interfacial heat transfer coefficient. The values of interfacial heat transfer coefficient increase as the pressure is increased varying from 0.383 $\mathrm{MW/m^2\,K}$ to 15.7 $\mathrm{MW/m^2\,K}$ for a pressure ranging from 0.01 atm to 1.0 atm, respectively and is reported in literature [8] for steam during DWC.

The total temperature difference between the vapor and the substrate surface is,

$$\Delta T = \Delta T_{\mathrm{i}} + \Delta T_{\mathrm{d}} \tag{7}$$

The minimum radius of the drops that can possibly grow for a given wall sub-cooling is [25],

$$r_{\min} = \frac{2T_{\mathrm{s}}\sigma}{H_{\mathrm{fg}}\rho\,\Delta T} \tag{8}$$

where, H_{fg}, ρ are the surface tension (N/m), latent heat of vaporization (J/kg) and density of the condensate ($\mathrm{kg/m^3}$) respectively. By combining Eqs. (5)–(7) we obtain,

$$\Delta T = \frac{q}{2\pi r^2 h_{\mathrm{i}}} + \frac{qr}{4\pi r^2 k_{\mathrm{c}}} \tag{9}$$

$$q = \Delta T 4\pi r^2 \left(\frac{1}{\frac{2}{h_{\mathrm{i}}} + \frac{r}{k_{\mathrm{c}}}}\right) \tag{10}$$

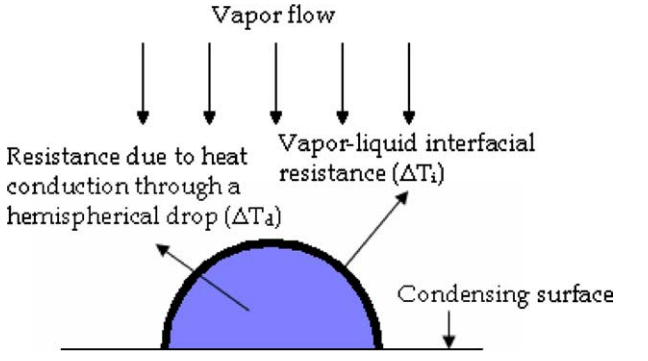

Fig. 1. Resistances involved to heat transfer through a hemispherical drop heat conduction through a hemispherical drop [4].

The rate of heat transfer through a hemispherical drop can also be expressed as,

$$q = \rho H_{\mathrm{fg}} 2\pi r^2 \frac{\mathrm{d}r}{\mathrm{d}t} \tag{11}$$

By equating Eqs. (10) and (11) the drop growth rate is given by,

$$G = \frac{\mathrm{d}r}{\mathrm{d}t} = \frac{2\Delta T}{\rho H_{\mathrm{fg}}}\left(\frac{1}{\frac{2}{h_{\mathrm{i}}} + \frac{r}{k_{\mathrm{c}}}}\right) \tag{12}$$

Let,

$$A_1 = \frac{2\Delta T}{\rho H_{\mathrm{fg}}} \tag{13}$$

$$A_2 = \frac{1}{k_{\mathrm{c}}} \tag{14}$$

$$A_3 = \frac{2}{h_{\mathrm{i}}} \tag{15}$$

By substituting Eqs. (13), (14) and (15) in Eq. (12) we obtain,

$$G = A_1\left(\frac{1}{A_2 r + A_3}\right) \tag{16}$$

Knowing G as a function of r, we now integrate Eq. (4) to give,

$$\int_{(Gn)_{\min}}^{Gn} \frac{\mathrm{d}(Gn)}{Gn} = \int_{r_{\min}}^{r} \frac{-\mathrm{d}r}{G\tau} \tag{17}$$

$$\int_{(Gn)_{\min}}^{Gn} \frac{\mathrm{d}(Gn)}{Gn} = -\frac{1}{A_1\tau}\left(\frac{A_2}{2}\left(r^2 - r_{\min}^2\right) + A_3(r - r_{\min})\right) \tag{18}$$

By solving the above equation we obtain,

$$n(r) = \frac{(Gn)_{\min}}{G}\exp\left(\frac{-1}{A_1\tau}\left(\frac{A_2}{2}\left(r^2 - r_{\min}^2\right) + A_3(r - r_{\min})\right)\right) \tag{19}$$

Because coalescence between drops is not considered in the foregoing derivation, Eq. (19) is valid only for the region where small drops grow mainly by direct condensation. For larger drops $N(r)$, the size distribution proposed by LeFerve and Rose is adopted here because of its simplicity and its agreement with the experimental data [4],

$$N(r) = \frac{1}{3\pi r^2 \widehat{r}}\left(\frac{r}{\widehat{r}}\right)^{-2/3} \tag{20}$$

where the expression for $\widehat{r}$ can be obtained as [5,27,28],

$$\widehat{r} = K_1\left(\frac{\sigma}{\rho g}\right)^{1/2} \tag{21}$$

with $K_1 = 0.4$ [27,28] and $N(r)$ is the population density of large drops in number per unit area per unit drop radius.

Where, r_{e} is the effective radius. This radius is equal to half the mean spacing between the active nucleation sites on the substrate surface. Assuming that the nucleation sites form a square array [2,3,29] which gives;

$$r_{\mathrm{e}} = \sqrt{\frac{1}{4N_{\mathrm{s}}}} \tag{22}$$

where, N_s is the number of nucleation sites on the condensing surface.

Eq. (19) gives the drop-size distribution for small drops $n(r)$ which grow mainly by direct condensation for the region where $r < r_e$ and Eq. (20) gives the drop-size distribution of larger drops $N(r)$ which grow due to coalescence for the region where, $r > r_e$.

With the boundary condition at $r = r_e$, $n(r) = N(r)$ enables one to express $(Gn)_{min}$ as a function of r_e. By applying the above boundary condition for Eq. (19) we obtain,

$$(Gn)_{min} = \frac{1}{3\pi r^2 \widehat{r}} \left(\frac{r}{\widehat{r}}\right)^{-2/3} G(r_e) \times \exp\left(\frac{1}{A_1\tau}\left(\frac{A_2}{2}\left(r_e^2 - r_{min}^2\right) + A_3(r_e - r_{min})\right)\right) \quad (23)$$

By substituting Eq. (23) into Eq. (19) the expression for $n(r)$ can be given as,

$$n(r) = \frac{1}{3\pi r^2 \widehat{r}} \left(\frac{r}{\widehat{r}}\right)^{-2/3} \left(\frac{A_2 r + A_3}{A_2 r_e + A_3}\right) \times \exp\left(\frac{1}{A_1\tau}\left(\frac{A_2}{2}\left(r_e^2 - r^2\right) + A_3(r_e - r)\right)\right) \quad (24)$$

For, $\tau = \frac{S}{A}$ the surface renewal rate S can be computed as follows:

$$S = \frac{A_d}{t} \quad (25)$$

where, t is the time taken by the large drop to sweep the substrate surface and A_d is the actual area of swept region due to large drops falling and can be expressed as [30],

$$A_d = \pi r_{max}^2 \sin\theta^2 \quad (26)$$

where, θ is the contact angle of the drop.

The steady state heat transfer rate per unit area of condenser surface during the process of dropwise condensation can be calculated from the below equation:

$$Q = \int_{r_{min}}^{r_e} q(r)n(r)\,dr + \int_{r_e}^{r_{max}} q(r)N(r)\,dr \quad (27)$$

4. Experimental verification

In order to study dropwise condensation two different types of SAM coatings have been used for experimentation. The experimental apparatus system is made of a boiler, chiller, vacuum pump, moisture trapper and the condensing chamber. Detailed descriptions of the experimental apparatus along with the uncertainty analysis involved are provided in the author's earlier publication [31].

4.1. SAM coating preparation

The ability to tailor the surface properties of the metal substrate using SAMs provides a new capability of controlling the behavior of working fluids on a heat transfer surface and can lead to significantly improved heat transfer rates.

4.1.1. Formation of an ultra thin film of n-octadecyl mercaptan on the surface by covalent bonding

We used a finely polished copper alloy (99.9% Cu, 0.1% P) tube with an outside diameter of 19.05 mm a wall thickness of 2.057 mm, and a length of 406.4 mm. The copper alloy tube was immersed in a 30% hydrogen peroxide (H_2O_2) solution for 8 h, while stirring using a stir bar. This would allow an oxide layer to be formed on the copper surface which would provide a stronger bonding between the condensing surface and the self-assembled mono-layer coating. The tube is then removed from the hydrogen peroxide solution and immersed in a 2.5 mM solution of *n*-octadecyl mercaptan in ethanol for 15 h. A thin film of the organic compound formed on the surface of the copper which was then washed with ethanol (99.9%) and dried. The organic film was produced by self-assembly of molecules attached to the metal oxide surface by covalent bonds and has a stronger bonding to the substrate surface due its higher electrostatic attraction.

4.1.2. Formation of an ultra thin film of stearic acid on the surface by hydrogen bonding

The surface of the copper alloy tube with the same dimensions mentioned above (in Section 4.1.1) was finely polished and placed in 30% hydrogen peroxide solution for 6 h at room temperature. The copper tube was removed from the H_2O_2 solution and left to dry for 20 min. Then the tube was placed in a 2.5 mM solution of stearic acid in hexane. After a period of eight hours the tube was removed from the organic acid solution and washed with hexane. The tube was left to air dry for three hours and then tested for the hydrophobic layer using water as the wetting solvent. The surface of the tube was hydrophobic and the layer was uniform. In this system the stearic acid molecules attach to the copper surface by hydrogen bonding to the oxide coating.

A CAM-100 type contact angle measurement apparatus (KSV Instruments, Finland) with an accuracy of $\pm 0.5°$ was used to measure the contact angles of liquids on the SAM coated plates at room temperature in order to assess the surface characteristics of the SAM coated surfaces. If the contact angle is less than 90° the liquid is said to wet the solid, and greater than 90° it is said to be non-wetting. Fig. 2 is the contact angle measurements for the copper alloy surface, *n*-octadecyl mercaptan coated surface (SAM-1), and stearic acid coated surface (SAM-2) before experimentation. Contact angle measurements were also measured for *n*-octadecyl mercaptan (after 500 h of operation) coated and stearic acid (after 10 h of operation) coated surfaces after the experiments were conducted. Fig. 3 shows the contact angle measured data after experiments for SAM-1 and SAM-2, respectively. The contact angle of water on the condensing surface has been used to predetermine the condensation mode [8].

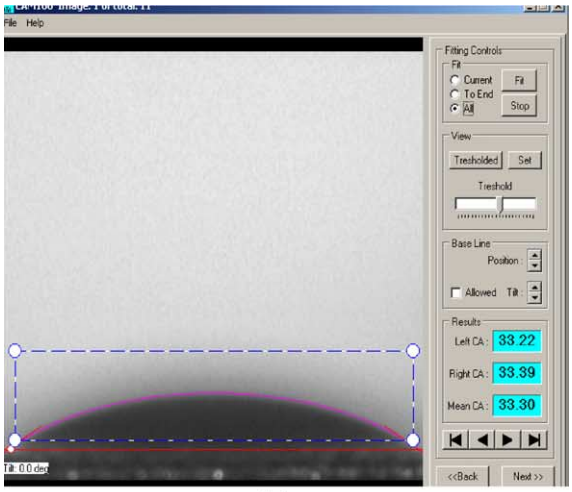

(a)

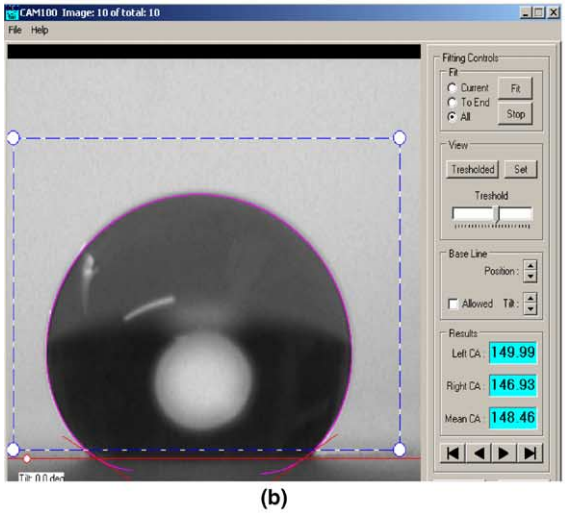

(b)

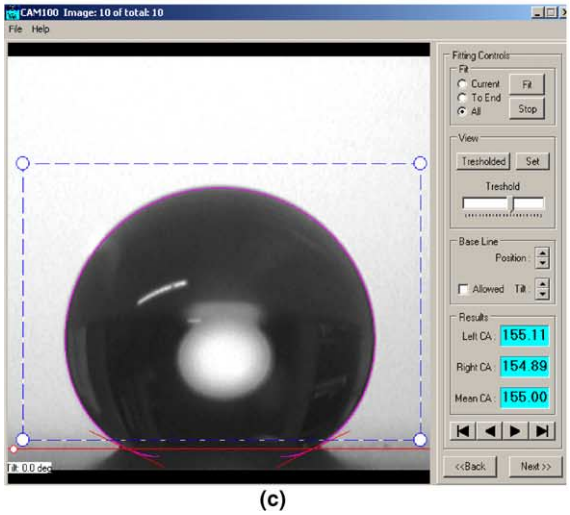

(c)

Fig. 2. Contact angle measurement for (a) copper alloy surface, (b) *n*-octadecyl mercaptan on the surface before experimentation and (c) stearic acid before experimentation.

5. Experimental data reduction

The coolant velocity in the tube was varied from 1.4 to 3.2 m/s, corresponding to Reynolds numbers ranging from

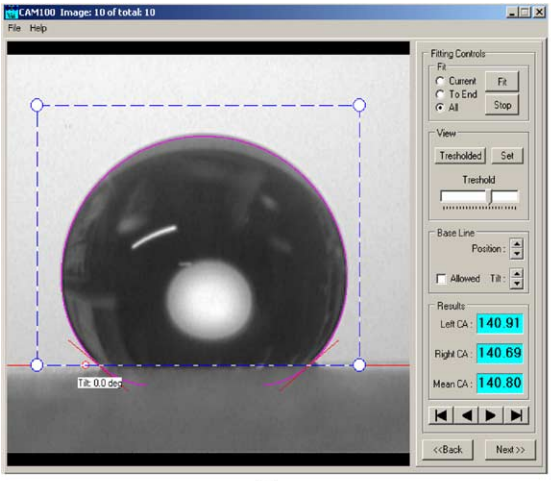

(a)

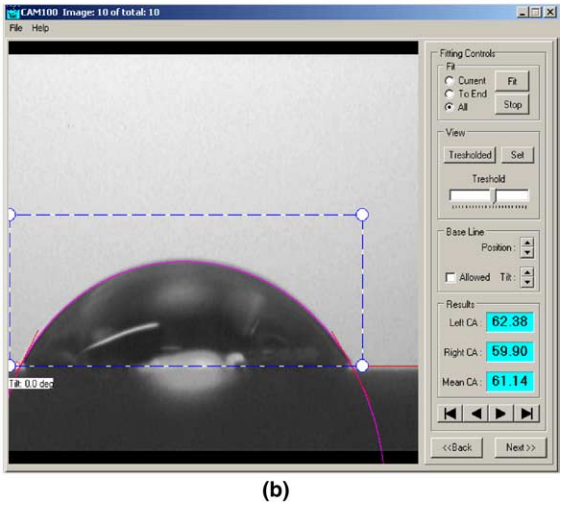

(b)

Fig. 3. Contact angle measurement for (a) *n*-octadecyl mercaptan and (b) stearic acid on the surface after experimentation.

19,500 to 45,100. The heat transfer rate to the condensation tube Q_w, was determined from the following equation:

$$Q_w = m_w c_p (T_o - T_i) \tag{28}$$

Q_w is used to calculate the overall heat transfer coefficient, U,

$$U = \frac{Q_w}{A_o \Delta T_{LMTD}} \tag{29}$$

$$\Delta T_{LMTD} = \frac{T_o - T_i}{\ln\left(\frac{T_s - T_i}{T_s - T_o}\right)} \tag{30}$$

The convective heat transfer coefficient, h_w, for cooling water inside the tube was determined by the following correlation, reported earlier for relatively short tubes [22]:

$$Nu = 0.062 Re^{0.75} Pr^{0.353} \tag{31}$$

The mean condensation heat transfer coefficient, h_c, on the outside of the tube was determined by subtracting the inside and wall thermal resistances from the overall thermal resistance, or

$$h_c = \frac{1}{\left(\frac{1}{U} - \frac{A_o}{A_i h_w} - A_o\left[\frac{\ln\left(\frac{d_o}{d_i}\right)}{2\pi \cdot l \cdot K}\right]\right)} \quad (32)$$

The surface sub-cooling temperature, ΔT, with an uncertainty of about 4% in the calculated value, was hence obtained from dividing the mean heat transfer rate, q, by the average condensation heat transfer coefficient.

$$q = \frac{Q_w}{A_o}, \quad \Delta T = \frac{q}{h_c} \quad (33)$$

6. Results and discussion

Every experimental run was kept operated at a constant pressure 33.86 kPa and 101.3 kPa for more than 2 h after reaching steady-state. All tests were repeated at least once on a different day. As a check, experimentally determined heat flux and condensation heat transfer coefficient, measured with this apparatus for pure FWC on a bare tube, compared well with the well known Nusselt correlation [10]. Excellent dropwise condensation was obtained on the SAM-1 surface for all the experiments conducted on it. SAM-2 surface sustained DWC for only 10 h of experimentation because it may be due to weak electrostatic attraction of hydrogen bonding used in stearic acid molecules to bond to the tube surface. Figs. 4 and 5 shows the variation of condensation heat transfer coefficient as a function of surface sub-cooling operated at pressures 33.86 kPa and 101.3 kPa. From the Figs. 4 and 5 it can be seen that condensation heat transfer rate was enhanced by a factor of three at 33.86 kPa pressure and by a factor of eight when operated at a pressure of 101.3 kPa when the condensing surface was coated with SAM-1, as compared to the values for film condensation on a bare copper–brass tube. It can be seen that the driving potential (or required temperature difference) using SAM-1 coating, was significantly reduced as compared to FWC for the applied input power. The improvement during DWC results primarily from the presence of numerous microscopic sized droplets on the hydrophobic surfaces that do not exist during FWC. Active sweeping of larger drops from above help continue the nucleation of small droplets on the surface, after a larger drop sweeps off the surface; the DWC cycle then repeats itself. This sweeping effect controls the size of drops on the lower part of the tube, as they are prevented from growing too large due to their coalescence into the sweeping drop. The heat transfer coefficients for atmospheric condition with no non-condensable gases, for all the runs were found to be greater than those under vacuum condition. Das et al. [23] reported a similar increase in dropwise heat transfer coefficient with increasing pressure, ratios of about 2.2–2.9 for SAM on copper and SAM on copper–nickel for a pressure ranging from 10 kPa to 100 kPa and also for a vertical copper surface. One possible explanation for the larger values in heat transfer rate may be due to the effect of interfacial heat transfer coefficient. Interfacial heat transfer coefficient of water vapor at atmospheric pressure is extremely high, being almost three orders of magnitude higher than the heat transfer coefficient of film condensation as reported in literature [8], and hence would have been the cause for high heat transfer rate in dropwise condensation at atmospheric pressure.

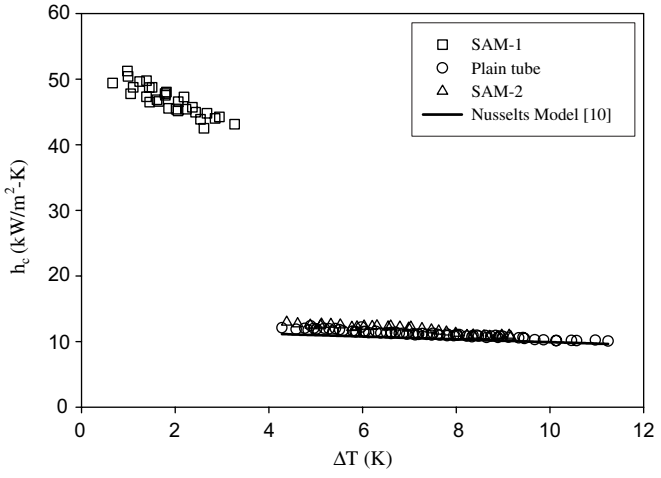

Fig. 4. Condensation heat transfer coefficient versus vapor to tube wall temperature difference during DWC of steam on coated tubes operated at 33.86 kPa.

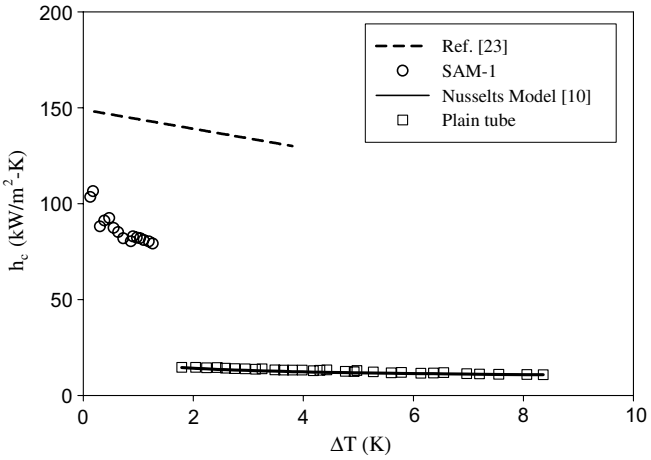

Fig. 5. Condensation heat transfer coefficient versus vapor to tube wall temperature difference during DWC of steam on coated tubes operated at 101.3 kPa.

The drop population density obtained from Eqs. (20) and (24) is plotted in Fig. 6. Eq. (20) gives the population density for small drops $n(r)$ which grow mainly by direct condensation and Eq. (24) gives the population density of larger drops $N(r)$ which grow due to coalescence. There was a very little notable variation in the drop population density when plotted as shown in Fig. 6 for different operated pressures (33.86 kPa and 101.3 kPa). From the Fig. 6 the left side region before r_e represents the population density for small drops $n(r)$ which grow mainly by direct condensation and the right side region after r_e represents the population density of larger drops $N(r)$ which grow due

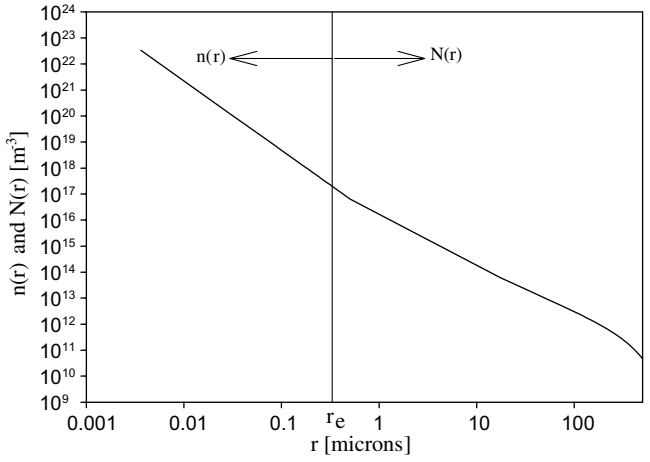

Fig. 6. Population densities of small and large drops as a function of drop radius (where $n(r)$ and $N(r)$ are the population density for small drops which grow mainly by direct and the population density of larger drops which grow due to coalescence, respectively).

to coalescence. The population density up to a drop radius before that of r_e, the rate of decrease in the drop population density is not as steep as the rate of the drop radius greater than r_e. This is because coalescence between drops starts taking place when the drop radius reaches r_e.

Fig. 7 shows the variation of heat flux, Q, as a function of surface sub-cooling, ΔT. From the Fig. 7 it can be seen that the driving potential or required temperature difference for the experiment using SAM-1 coating at both the operating pressures of 33.86 kPa and 101.3 kPa is reduced compared to FWC for the applied input power. The experimental data for SAM-2 are not shown in the Fig. 7 as it showed FWC and results were in the same range to that obtained for FWC. The number of nucleation sites on a surface were normally in the range of 10^9–10^{13} sites/m^2 as reported in the literature [32,33]. The number of nucleation sites ($N_s = 10^9$ sites/m^2) used in this computation are within the range mentioned above and is the main driving parameter in obtaining the heat flux. It is also been shown

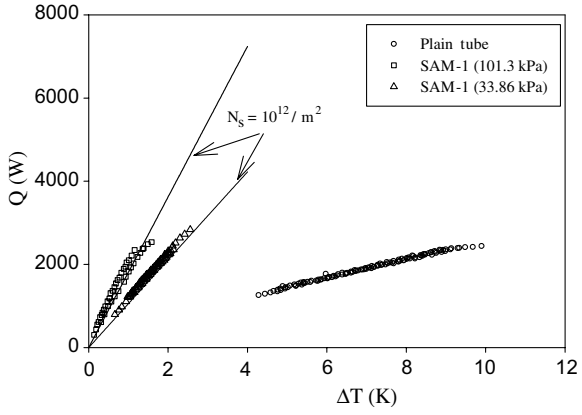

Fig. 7. Heat flux versus vapor to tube wall temperature difference (where N_s, is the number of nucleation sites/m^2).

by researchers [32,33] that the drop distribution and heat flux are dependent on the density of active nucleation sites on the substrate surface. The value of the maximum drop radius (1.5 mm) can be obtained by experimental observation and by knowing the contact angle of the drop made with the condensing surface from which the surface renewal rate due to large falling drops is calculated. Heat flux obtained from the theoretical model (Eq. (27)) is also plotted in Fig. 7. Mentioned earlier one principle explanation for the increase in heat transfer rate at higher pressures was due to increase in interfacial heat transfer rate as reported in literature [8] the values of interfacial heat transfer coefficient increase as the pressure is increased varying from 0.383 MW/m^2 K at 0.01 atm to 15.7 MW/m^2 K at 1.0 atm, respectively for steam during DWC. The increase in values of interfacial heat transfer coefficient due to increasing pressures was considered into the model and from Fig. 7 it can be seen that there is a very good agreement with the experimental data obtained when operated at pressures of 33.86 kPa and 101.3 kPa, respectively for a given number of nucleation sites.

7. Conclusions

The effects of SAM coatings on the condensation heat transfer characteristics were investigated experimentally and theoretically. The conclusions of this study can be summarized as follows:

1. It is evident that from the results that there is an enhancement up to three times in condensation heat transfer rate for dropwise condensation when operated at vacuum condition and an enhancement of eight times when operated at atmospheric condition over filmwise condensation respectively.
2. In the current research experiments (Fig. 4) were carried out using SAM-1 (*n*-octadecyl mercaptan) coating for 500 h and it showed good dropwise condensation. Stearic acid (SAM-2) coated tube had a contact angle of 155° (drop wise) but when the experiment was conducted it gradually turned to film wise condensation mode and had a contact angle of 61.1° after the experimentation, which is due to weak electrostatic attraction of hydrogen bonding to the tube surface and would have been dissolved when operated at high temperatures. From the studies it is found that bonding of the SAM coating to the metal substrate plays an important role in maintaining long term DWC. Covalent bonding is better than the hydrogen bonding of the SAM to the metal substrate due to its high electrostatic attraction.
3. One possible explanation for the larger values in heat transfer rate may be due to the effect of interfacial heat transfer coefficient. Interfacial heat transfer coefficient of water vapor at atmospheric pressure is extremely high at atmospheric pressure when compared to vacuum pressure (lower than at atmospheric pressure) in the absence of non-condensable gases as reported in

literature [8], and hence would have been the cause for high heat transfer rate in dropwise condensation at atmospheric pressure.

4. Population balance concept was used to derive a theoretical formula to predict the drop-size distribution of small drops which grow mainly by direct condensation. All the important resistances to heat transfer such as the heat conduction through the drop, vapor–liquid interface are considered in developing this model.
5. By, knowing the contact angle of the drop made with the condensing surface and the maximum drop radius (1.5 mm) the sweeping effect of large falling drops could be calculated. The number of nucleation sites used in this computation were within the range as reported in the literature and is the main driving parameter in determining the heat flux.
6. In general, a SAM system with a long-chain, hydrophobic group is nano-resistant, meaning that such a system forms a protective hydrophobic layer with negligible heat transfer resistance but a much stronger bond. The durability of the SAM coating is strongly dependent upon the bonding between the coating and the condensing surface. As, of now after 500 h of operation the SAM coated surfaces still exhibited good dropwise characteristics and further durability tests are being carried out.

Acknowledgements

The authors are grateful to the financial support provided by the US DOE/National Technology Energy Laboratory (NETL, DE-FG26-02NT41543) and Nevada Ventures Nanoscience Program. Special thanks go to Dr. B.D. Wood of Utah State University and Dr. T.W. Bell of Chemistry, UNR. Laboratory help of Ms. S. Govindaraju was helpful.

References

[1] W.H. Wu, J.R. Maa, On the heat transfer in dropwise condensation, Chem. Eng. J. 12 (1976) 225–231.
[2] J.R. Maa, Drop size-distribution and heat flux of dropwise condensation, Chem. Engr. J. 16 (1978) 171–176.
[3] M. Abu-Orabi, Modeling of heat transfer in dropwise condensation, Int. J. Heat Mass Transfer 1 (41) (1998) 81–87.
[4] N. Fatica, D.L. Katz, Dropwise condensation, Chem. Engr. Prog. 45 (11) (1949) 661–674.
[5] E.J. Le Ferve, J.W. Rose, A theory of heat transfer by dropwise condensation, in: Proceedings of 3rd International Heat Transfer Conference, vol. 2, Chicago, 1966, pp. 362–375.
[6] J.W. Rose, L.R. Glicksman, Dropwise condensation- the distribution of drop sizes, Int. J. Heat Mass Transfer 16 (1973) 411–425.
[7] J.W. Rose, Dropwise condensation theory, Int. J. Heat Mass Transfer 24 (1981) 191–194.
[8] I. Tanasawa, Advances in condensation heat transfer, Adv. Heat Transfer 21 (1991) 55–139.
[9] J.G. Collier, Convective Boiling and Condensation, second ed., McGraw-Hill, New York, 1981.
[10] S. Kakac, H. Liu, Heat Exchangers, CRC Press, New York, 1998.
[11] H. Tanaka, A theoretical study of dropwise condensation, Trans. ASME J. Heat Transfer 97 (1975) 72–78.
[12] H. Tanaka, Further development of dropwise condensation theory, Trans. ASME J. Heat Transfer 101 (1979) 603–611.
[13] R.A. Erb, E. Thelen, Dropwise condensation characteristics of permanent hydrophobic systems, US Office of Saline Water R&D Report No. 184, 1966, pp. 54–57.
[14] D.W. Woodruff, J.W. Westwater, Steam condensation on electroplated gold: effect of plating thickness, Int. J. Heat Mass Transfer 22 (1979) 629–632.
[15] D.W. Woodruff, J.W. Westwater, Steam condensation on various gold surfaces, ASME J. Heat Transfer 103 (1981) 685–692.
[16] G.A. O'Neill, J.W. Westwater, Dropwise condensation of steam on electroplated silver surfaces, Int. J. Heat Mass Transfer 27 (9) (1984) 1539–1549.
[17] P.J. Marto, D.J. Looney, J.W. Rose, A. Wanniarachchi, Evaluation of organic coatings for the promotion of dropwise condensation of steam, Int. J. Heat Mass Transfer 29 (8) (1986) 1109–1117.
[18] K.M. Holden, A. Wanniarachchi, P.J. Marto, D.H. Boone, J.W. Rose, The use of organic coatings to promote dropwise condensation of steam, ASME J. Heat Transfer 109 (1987) 768–774.
[19] T. Haraguchi, R. Shimada, S. Kumagai, T. Takeyama, The effect of polyvinylidene chloride coating thickness on promotion of dropwise steam condensation, Int. J. Heat Mass Transfer 34 (12) (1991) 3047–3054.
[20] X. Ma, D. Xu, J. Lin, Dropwise condensation on super thin polymer surface, J. Chem. Indust. Eng. (China) 44 (2) (1993) 165–170.
[21] Q. Zhao, D. Zhang, J. Lin, Surface material with dropwise condensation made by ion implantation technology, Int. J. Heat Mass Transfer 34 (11) (1991) 2833–2835.
[22] X. Ma, J. Chen, D. Xu, J. Lin, C. Ren, Z. Long, Influence of processing conditions of polymer film on dropwise condensation heat transfer, Int. J. Heat Mass Transfer 45 (2002) 3405–3411.
[23] A.K. Das, H.P. Kilty, P.J. Marto, B.G. Andeen, A. Kumar, The use of an organic self-assembled monolayer coating to promote dropwise condensation of steam on horizontal tubes, ASME J. Heat Transfer 122 (2000) 278–286.
[24] A.D. Randolph, M.A. Larson, Theory of Particulate Processes, second ed., Academic Press Inc., New York, 1988.
[25] C. Graham, P. Griffith, Drop size distributions and heat transfer in dropwise condensation, Int. J. Heat Mass Transfer 16 (1973) 337–346.
[26] B.B. Mikic, On mechanism of dropwise condensation, Int. J. Heat Mass Transfer 12 (1969) 1311–1323.
[27] E.J. Le Ferve, J.W. Rose, An experimental study of heat transfer by dropwise condensation, Int. J. Heat Mass Transfer 8 (1965) 1117–1133.
[28] J.W. Rose, Dropwise condensation theory and experiment: a review, in: Proceedings Institute of Mechanical Engineers, vol. 216, Part A: Journal of Power and Energy, 2002, pp. 115–128.
[29] C. Yamali, H. Merte Jr., A theory of dropwise condensation at large sub-cooling including the effect of the sweeping, Heat Mass Transfer 38 (2002) 191–202.
[30] G. Koch, K. Kraft, A. Leipertz, Parameter study on the performance of dropwise condensation, Rev. Gen. Therm. 37 (1998) 539–548.
[31] S. Vemuri, K.J. Kim, B.D. Wood, S. Govindaraju, T.W. Bell, The effect of nano-tailored surfaces on steam condensation, in: Proceedings of IMECE 2003, Washington, DC, 2003, IMECE2003-43083.
[32] R.L. Glicksaman, W.A. Hunt Jr., Numerical simulation of dropwise condensation, Int. J. Heat Mass Transfer 15 (1972) 2251–2269.
[33] L.J. McCormick, J.W. Westwater, Nucleation sites for dropwise condensation, Chem. Eng. Sci. 20 (1965) 1021–1036.